XVI IMEKO World Congress
Measurement - Supports Science - Improves Technology - Protects Environment ... and Provides Employment - Now and in the Future
Vienna, AUSTRIA, 2000, September 25-28

PHASE-DETECTION WAVELENGTH-SCANNING INTERFEROMETRY

J. Kato and I. Yamaguchi
Optical Engineering Laboratory, RIKEN (Inst. Phys. Chem. Res.)
2-1, Hirosawa, Wako, Saitama, Japan

Abstract: We have realized an accurate height measurement for discontinuous shape by using the wavelength scanning interferometry combined with phase-shifting technique. It is based on detection of phase variation slope along the wavenumber axis at each pixel of a CCD camera that takes a number of phase-shifted interferograms using a PZT mirror. By using a tunable laser diode with wavelength-scanning range of 8 nm and scanning step of 0.2 nm, a height standard deviation of 40 nm could be obtained for the depth of ± 0.75 mm. This technique was applied to profile measurements of an aspherical mirror and rough-surface objects.
Keywords: Wavelength-scanning interferometry, Phase analysis, Profilometry

1 INTRODUCTION

Interferometry have been usefully applied to a high-accurate shape measurement of specular surface. This technique, however, has an uncertainty problem in fringe-order decision when the measured surface contains discontinuous steps whose height differences are larger than a half wavelength. On the other hand, the demand for precise evaluation of complex shapes including the discontinuous step, such as binary diffractive optical elements and minute micro-machined parts, has recently been increased so that the interferometry was also requested to deal with these targets. For these purposed, the wavelength-scanning interferometry (WSI) has been developed.[1-3] When a laser wavelength is linearly changed in an interferometer, the interference intensity shows periodic modulations whose frequency is proportional to the optical path difference (OPD). This is a principle of the WSI which can be applied to profile measurements of both specular and rough surfaces having discontinuous steps higher than a half wavelength. Usually the modulation frequency is analyzed by the fast Fourier transformation (FFT) technique or the fringe counting techniques.[1,3] In these techniques, however, a wide range of the wavelength scanning more than 20 nm is necessary for attaining an accuracy of μm order. Additionally, the measurement around the zero-path position and an identification of the sign of the measured height are also difficult.

To overcome these problems, we introduce the phase-analysis into the wavelength-scanning interferometry (Phase-detection wavelength-scanning interferometry: PWSI).[4] By deriving the phase-variation slope against the wavelength change at each pixel, the height map of the object can be directly calculated including the sign of OPD. The accuracy and the performances of this method have been estimated by experiments, in which a tunable laser diode and a conventional PZT (piezoelectric transducer) mirror are used. By extending the wavelength-scanning rage to 8 nm and suppressing the several error sources of this technique, which includes the influences of reflection from the back-surface of optical elements, the height measurement accuracy could be improved to several-tenth nm. With this improvement, we could realize the unification of measurement results between the WSI and the conventional single-wavelength interferometry (SWI). We have applied this technique to profile measurement of an aspherical mirror and rough surfaces. Because this technique depends on the phase-slope measurement against the wavelength-change at each pixel, the height measurement can be conducted under the sub-Niquist condition of fringe density, in which intensity distribution of fringes more than one is integrated in a CCD pixel. If the height error caused by this effect is small enough, the measurable area for specular surface can be extended. We have also examined the dependencies of height error on the fringe densities in the experiments.

2 PRINCIPLES

When the wavelength is changed by $\Delta\lambda$ from the initial wavelength λ_0 in a Michelson interferometer with a PZT mirror, resultant fringe intensity observed at the position (x, y) is expressed as

$$I_i(x,y,\Delta l) = I_o + I_r + 2\sqrt{I_o I_r}\, g(x,y)\cos\left[f(x,y,l_0) + \Delta f(x,y,\Delta l) + y_i\right] \quad \text{and} \tag{1}$$

$$\Delta f\,(x,y,\Delta\, l) = -2p\,\frac{h(x,y)\,\Delta\, l}{l_0^2} \tag{2}$$

where g, f, and y_i are the fringe contrast, the initial phase, and the phase-shift introduced by movement of the PZT mirror, respectively. The slope of the phase variation $\Delta f\,(x,y,\Delta\, l)/\,\Delta l$ is shown to be proportional to the OPD $h(x, y)$. Therefore, by changing the wavelength by a known amount and taking the difference between the adjacent phase-maps, the bias term $f\,(x,y,l_0)$ is eliminated and the phase-slope, which is proportional to the object height map, is derived through linear least-squares fitting at each pixel. The basic procedure of data-acquisitions for this technique is illustrated in Fig.1.

For the phase-analysis, the conventional five-step phase-shifting algorithm was used and the phase-map at each wavelength was derived by using the next relations,

$$f\,(x,y,l_0) + \Delta f\,(x,y,\Delta\, l) = \arctan\frac{2(I_2 - I_4)}{-I_1 + 2I_3 - I_5} \tag{3}$$

The contrast g is also derived and is used as a criterion for removing the low-modulation pixels in the height-calculation.

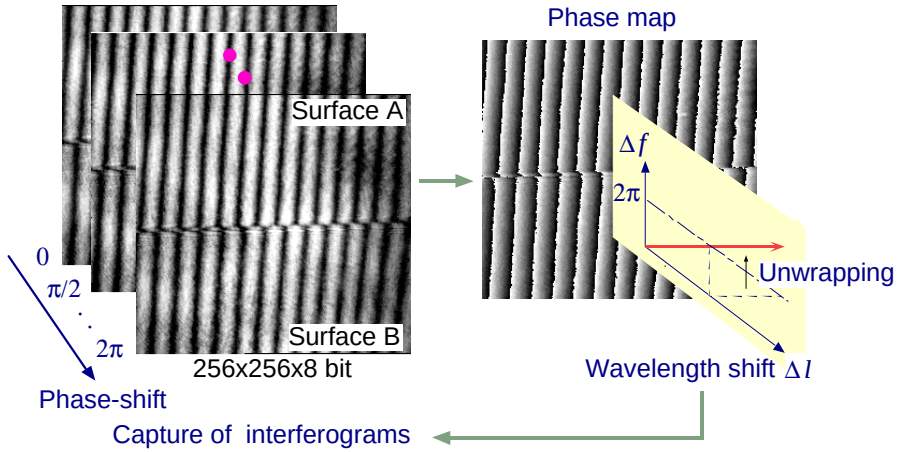

Figure 1. Basic procedure of data-acquisitions in PWSI.

3 EXPERIMENTS

3.1 Experimental setup

Figure 2 shows the optical arrangement used in experiments. A tunable LD (SDL TC-40, wavelength tuning range 772–780 nm, output power 500 mW) was used as a light source. The emitted beam was collimated and is introduced into a Michelson interferometer. The beam is divided by a cube beam splitter into the reference and the object beams which are reflected by a reference mirror M1 and an object and combined to form an interference pattern on a CCD camera. For phase measurement, the reference mirror M1 is displaced with a PZT controlled by a computer for supplying the phase-shift of $\pi/2$ rad corresponding to the center wavelength of the LD (776 nm). A polarizer PL is inserted in front of the CCD camera to control the intensity ratio between the reference and the object beams in measurements of rough-surface objects. Minimum wavelength scanning step was set to 0.2 nm. This leads to measurable OPD range of ±0.75 mm. In the signal processing for height measurement, five interferograms (256x256 pixels, 8 bits) with mutual phase shift of $\pi/2$ are sequentially captured in a frame grabber after each wavelength-shift by the LD. This procedure is repeated over total wavelength scanning of 8

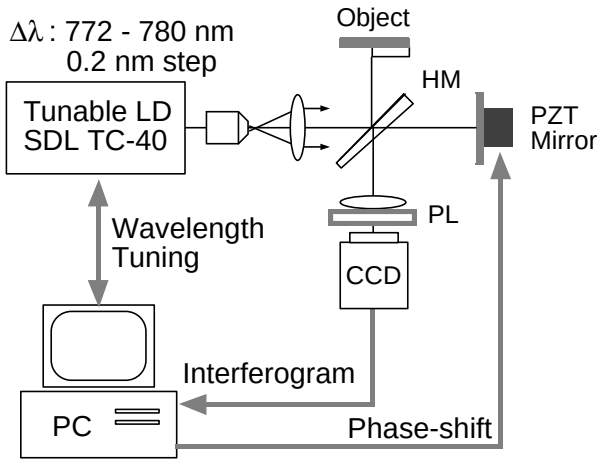

Figure 2. Experimental setup.

nm and the phase slope at each pixel is calculated via phase-unwrapping and the linear least squares fitting procedures.

For suppressing the influence of back-surface reflections of each optical element, the surfaces were AR-coated for 778 nm, and a plate-type half mirror was used as beam-splitter. Actually, maximum error was found to be introduced by multiple reflections between a glass-plate located in front of the CCD array and the array itself. To eliminate this influence, we adopted the special CCD camera (Hitachi Denshi Co. KP-2M) from whom the all face-plates were removed.

3.2 Error evalutation and unification with a SWI result

First a step gauge of 10.02±0.015 μm height was measured for estimating the accuracy of this technique. Figure 3 (a) and (b) show an example of obtained phase-slope curve against both of steps of the gauge with different OPD's and the dependencies of the wavelength-scanning range on the height deviations, which is calculated from the linear-square evaluations of phase-slopes, before and after improvement of the optical setup. Before the improvements (experiment #1), a cube-type beam splitter and a CCD camera with a face-plate glass were used. It is clearly shown that the measurement error decreases for the large wavelength change as expected. However, the decrease of the error is stopped at order of 0.5 μm, which is 10^2 times larger than the expected minimum error obtained by a numerical simulation in ideal conditions. While after the improvement (experiment #2) the error can be suppressed to reach the order of 10 nm. This deviation is ten times better than that obtained by the conventional frequency-analysis in the wavelength scanning interferometry. This result shows that the suppression of back-reflection by optical components is significantly effective for this method. Meanwhile, the final height deviation less than 0.1 μm makes it possible to unify the measurement results by the PWSI with that by the conventional interferometric measurement (SWI).

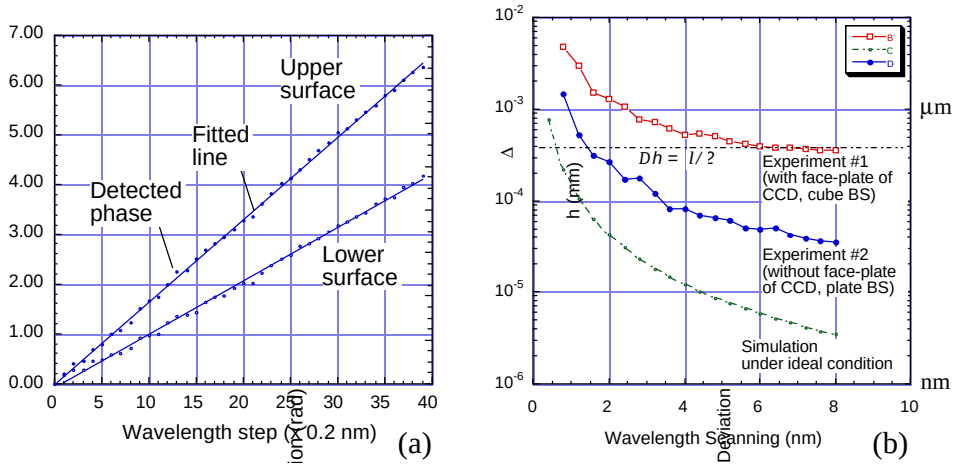

Figure 3. Height measurement results for 10 μm step gauge: (a) Phase-slope obtained on both surfaces of the step gauge, (b) dependence of wavelength-scanning range on rms errors in height measurement before and after improvement of the optical setup.

Figure 4 shows the unification procedure and results of the height maps obtained by the PWSI and the SWI. The three-dimensional representation of the final height map is also shown in Fig. 5. The resultant mean height-difference was 10.1 μm and the standard deviation for the height measurement becomes same as that obtained with the conventional interferometry. Although the same result can be obtained with the multiple-wavelength synthetic interferometry, any *a priori* information on the nominal height of the measured step is not necessary in the present technique.

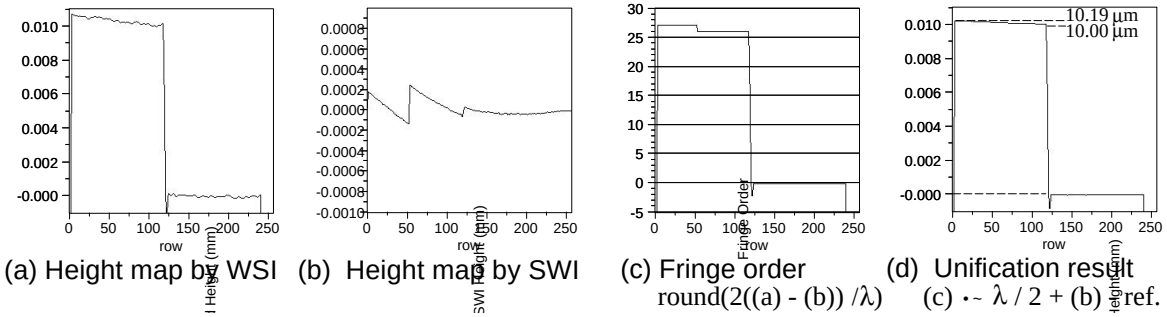

(a) Height map by PWSI (b) Height map by SWI (c) Fringe order round(2((a) - (b)) /λ) (d) Unification result (c) ･~ λ / 2 + (b) ref. err.

Figure 4. Unification of height maps of 10 μm step-gauge obtained by phase-detection WSI and SWI (Cross-sectional view).

3.3 Rough surface measurement

Another advantage of the WSI is height measurement of rough surface objects. The accuracy improvement in the PWSI is also effective in this application. As an example of the rough surface, we measured the rear-surface of one-yen coin in Fig. 6. Because this surface is consist of rough and quasi-specular surfaces as showin in Fig. 6 (a), the balance of intensity ratio between the reference and the object beams is difficult. We controlled the ratio by utilizing the minute change of polarization state for diffused light from a rough surface. The orientation of the polarizer PL placed in front of the CCD camera (in Fig. 2) was adjusted to cut almost of linear polarization from the specular surface and pass through the minute depolarized component from the rough surface. Using this technique, the profile over the total area could be obtained as shown in (b). From the cross sectional profile in Fig. 6 (c), the height deviation on the rough surfaces is order of 10 µm, which is adequate considering the roughness of the surface. In rough surface measurement, many pixels becomes unmeasurable because of speckle pattern generation. The appropriate filtering has to be developed to improve the measurement results.

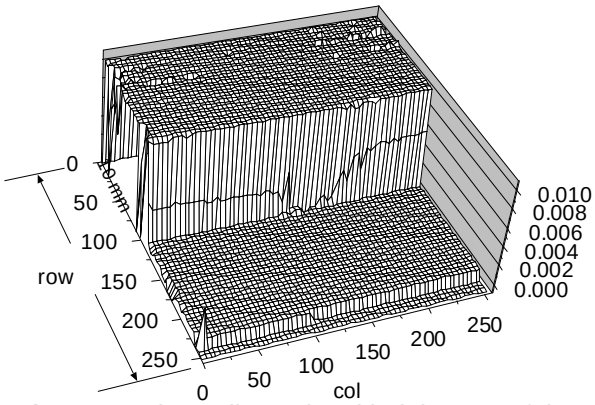

Figure 5. Three-dimensional height map of the step-gauge of 10 µm after the unification procedure.

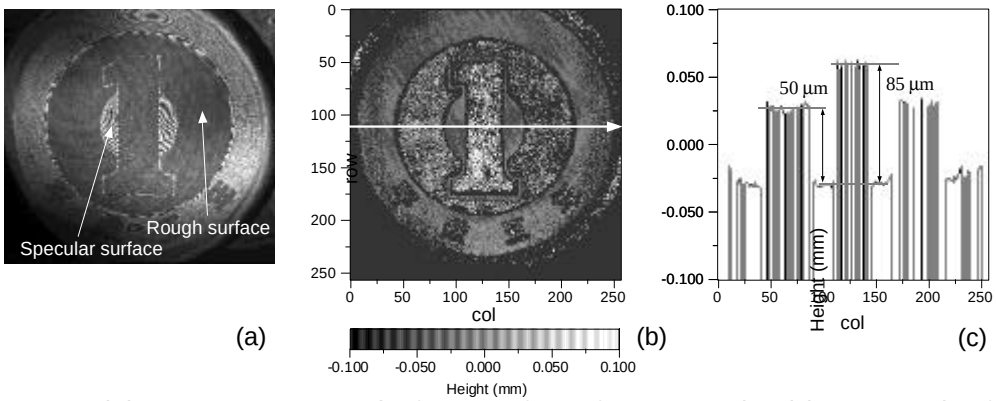

Figure 6. Height measurement result of rear-surface of one-yen coin: (a) an example of interferogram, (b) gray-level representation of height-map obtained with the PWSI, and (c) the horizontal cross-section of (b).

3.4 Measurement performance in sub-Nyquist condition

The PWSI is principally based on a pixel-by-pixel analysis. Hence, even if the fringe density becomes higher than the pixel pitch of the CCD camera (sub-Nyquist condition), the change of average phase against the wavelength change might be detectable as same as sub-Nyquist interferometry (SNI)[6]. By using this feature, we can expect to enlarge the measurable area in aspherical shape measurements. To examine the performance of the PWSI in the sub-Nyquist condition, the computer simulation was conducted by calculating the ideal fringe patterns for each wavelength step and processing them with the same analysis in the former experiments. To obtain the correct fringe pattern including the integration effect of dense fringe in a CCD pixel, the two-dimensional Gauss-Chebychev integration has been adopted. The measurement of a cylindrical wavefront with 1600 mm of curvature radius was assumed in the simulation. Figure 7 shows the obtained wavefront shape and the residual error from the ideal one under the full aperture condition (aperture size / picth = 1). In the result, the some unmeasurable regions appear near positions ±5 and 10 mm. However, the wavefront shape can be obtained with the accuracy more than ±0.2 µm expect these regions. These unmeasurable regions are caused at the part where the fringe modulation becomes significantly low. Even if avoiding these parts in measurement, we can expect the accuracy of sub-µm over the area of two times larger than the normally resolved part that satisfies the Nyquist condition.

To confirm this performance in the real experiment, we applied the PWSI to profile measurement of a grinded toric mirror. Figure 8 shows the measurement result of a toric-surface whose radii of

principal curvatures are 560 and 1960 mm respectively and whose rms roughness is about 0.3 μm. An example of the phase distribution used for the height calculation is shown in Fig.8 (a) and the obtained profile is shown in (b) and (c). Although the fringe density becomes higher than the pixel pitch of the CCD camera, the surface profile could be obtained over wider area than that obtained by the normal interferometry. The unmeasurable part could not be found in this result, whose reason might be that the ratio of pixel size and pich of the used CCD camera was less than one. The effect of the ratio on the measurement performance and the tendency of the height error must be studied more.

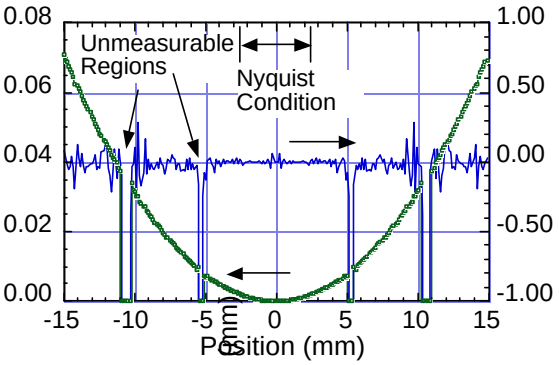

Figure 7. Simulation result of the PWSI under the sub-Nyquist condition for fringe density.

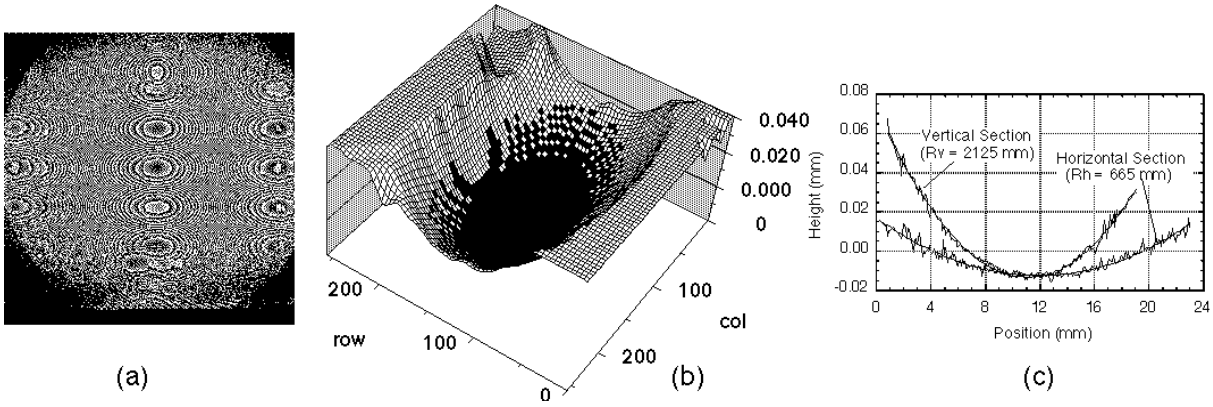

Figure 8. Measurement results of the grinded toric-surface: (a) a phase-map used for height calculation, (b) 3-D representation of the profile, and (c) the cross-section for principal directions.

4 CONCLUSIONS

The phase-shifting technique has been introduced to the wavelength scanning interferometry. The experimental results have shown more accurate height measurement with a narrower scanning range than in the intensity-based analysis. This technique could be applied to profile measurements of aspherical surfaces located across the zero-OPD position without increase of measurement errors. The data-acquisition time can be accelerated by using the optimized sampling based on the exponential sequence. [6] The possibility of enlargement of the measurement area using the sub-Nyquist characteristics is another advantage of this technique and to be useful in the measurement of complex object including the step and the aspherical surfaces.

REFERENCES

[1] M. Takeda and H. Yamamoto, "Fourier-transform speckle profilometry: three-dimensional shape measurements of diffuse objects with large height steps and or spatially isolated surfaces," *Appl. Opt.* **33** (1994) 7829-7837.
[2] T. H. Barnes, T. Eiju and K. Matsuda, “Rough surface profile measurement using speckle optical frequency domain,” *Optik*, **103** (1996) 93-100.
[3] S. Kuwamura and I. Yamaguchi, "Wavelength scanning profilometry for real-time surface shape measurement," *Appl. Opt.* **36** (1997) 4473-4482.
[4] J. Kato, and I. Yamaguchi, "Phase-shifting fringe analysis for laser diode wavelength-scanning interferometer," *Opt. Rev.* **7** (2000) 158-163.
[5] J. E. Greivenkamp, “Syb-Nyquist interferometry,” *Appl. Opt.* **26** (1987) 5245-5258.
[6] L. Paulsson, M. Sjödahl, J. Kato, and I. Yamaugchi, “Temporal phase unwrapping applied to wavelength-scanning interferometry,” to be appeared in *Appl. Opt.*

AUTHORS: J. KATO and I. YAMAGUCHI, Optical Engineering Laboratory, RIKEN (The Institute of Physical and Chemical Research), 2-1 Hirosawa, Wako, Saitama, 351-0198, Japan, Phone Int +81-48-462-1111, Fax Int +81-48-462-4653, E-mail: kato@optsun.riken.go.jp